Available online at www.sciencedirect.com
SCIENCE DIRECT®
Solar Energy 75 (2003) 511–524
SOLAR ENERGY
www.elsevier.com/locate/solener

Thermal and technical analyses of solar chimneys

M.A. dos S. Bernardes [a,*], A. Voß [a], G. Weinrebe [b]

[a] *Institut für Energiewirtschaft und Rationelle Energieanwendungen, Universität Stuttgart, Heßbrühlstraße 49a, D-70565 Stuttgart, Germany*
[b] *Schlaich Bergermann und Partner, Hohenzollernstr. 1, D-70178 Stuttgart, Germany*

Received 18 September 2002; received in revised form 15 August 2003; accepted 15 August 2003

Abstract

An analysis for the solar chimneys has been developed, aimed particularly at a comprehensive analytical and numerical model, which describes the performance of solar chimneys. This model was developed to estimate power output of solar chimneys as well as to examine the effect of various ambient conditions and structural dimensions on the power output. Results from the mathematical model were compared with experimental results and the model was further used to predict the performance characteristics of large-scale commercial solar chimneys. The results show that the height of chimney, the factor of pressure drop at the turbine, the diameter and the optical properties of the collector are important parameters for the design of solar chimneys.

1. Introduction

A solar chimney is a solar power generating facility, which uses solar radiation to increase the internal energy of air flowing through the system, thereby converting solar energy into kinetic energy. The kinetic energy from the air is then transformed in electricity by use of a suitable turbine. A solar chimney consists of three main components: (1) the solar collector or the greenhouse, (2) the chimney, and (3) the turbine (Fig. 1). The collector, supported a few meters above the ground, is covered by a transparent glazing. Its main objective is collecting solar radiation to heat up the air mass inside it. Buoyancy drives the warmer air into the chimney, which is located at the centre of the collector. A turbine is set in the path of the airflow to convert the kinetic energy of the flowing air into electricity. The collector can be equipped with a water-storage system (4) to increase the power production during the night.

The solar chimney was originally proposed by Professor J. Schlaich of Stuttgart in 1968. In 1981 began the construction on a pilot plant in Manzanares, Spain. A 50 kW experimental plant was built which produced electricity for eight years, thus proving the feasibility and reliability of this novel technology. The chimney tower was 194.6 m high and the collector had a radius of 122 m. It produced an upwind velocity of 15 m/s under no load conditions. Operating costs of this chimney were minimal. Fundamental investigations for the Spanish system were reported by Haaf et al. (1983) in which a brief discussion of the energy balance, design criteria, and cost analysis was presented. In a later study, Haaf (1984) reported preliminary test results of the plant built in Spain. Castillo (1984) presented a new chimney design with a new structure of the chimney building supported by a hot-air balloon. Mullet (1987) presented an analysis to derive the overall efficiency of the solar chimney. Padki and Sherif conducted an investigation of the viability of solar chimneys for medium-to-large scale power production, 1989a and power generation in rural areas, 1989b. Schlaich et al. (1990) studied the transferability from the experimental data of the prototype in

* Corresponding author. Address: Centro Federal de Educacao Tecnologia de Minas Gerais, Departamento de Engenharia Mecanica, Av. Amazonas 7675 Nova Gameleira, 30510-000 Belo Horizonte, Minas Gerias, Brazil. Tel.: +55-31-3319-5208; fax: +55-31-3319-5248.
E-mail address: marcobernardes@des.cefetmg.br (M.A. dos S. Bernardes).

0038-092X/$ - see front matter © 2003 Elsevier Ltd. All rights reserved.
doi:10.1016/j.solener.2003.09.012

Nomenclature

Latin symbols

A	area [m^2]
b	thermal penetration coefficient [$W s^{1/2} K^{-1} m^{-2}$]
c_p	specific heat [$J kg^{-1} K^{-1}$]
c_w	friction factor [–]
f	Fanning friction factor [–]
G	gravitational acceleration, 9.80665 [$m s^{-2}$]
H	incident solar radiation [$W m^{-2}$]
h	heat transfer convection coefficient [$W m^{-2} K^{-1}$]
H_k	chimney height [$W m^{-2}$]
h_r	radiation heat transfer coefficient [$W m^{-2} K^{-1}$]
h_{rs}	sky radiation heat transfer coefficient [$W m^{-2} K^{-1}$]
h_w	wind convection heat transfer [$W m^{-2} K^{-1}$]
k	thermal conductivity [$W m^{-1} K^{-1}$]
k_r	height of roughness [m]
L, L_w	length of collector, thickness of the water-storage system [m]
$\dot{m}$, m	mass flow rate of air stream [$kg s^{-1}$], mass [kg]
Nu	Nusselt number [–]
p, p_∞, p_t	pressure, ambient air pressure, air pressure inside the chimney [Pa]
P	power [W]
Pr	Prandtl number [–]
q	heat transferred to air stream [$W m^{-2}$]
r	radius [m]
Ra	Rayleigh number [–]
Re	Reynolds number [–]
R_l	ideal gas constant, 287.05 $J kg^{-1} K^{-1}$
S	absorbed solar radiation [$W m^{-2}$]
t	time [s]
T	temperatures [K]
T_∞, T_{dp} T_s	ambient, dew point temperature, sky temperature [K]
$T_{f,i}$, $T_{f,o}$	inlet, outlet temperature [K]
T_t	air temperature inside the chimney [K]
U	heat transfer coefficient [$W m^{-2} K^{-1}$]
w	velocity [$m s^{-1}$]
x	factor of pressure drop at the turbine [–]

Greek symbols

α	thermal diffusivity [$m^2 s^{-1}$]
α_1, α_2, α_3, α_4	first cover absorptivity, second cover absorptivity, transparent plastic film absorptivity, absorber absorptivity [–]
$\Delta p_{friction}$	friction loss [Pa]
Δp_{tot}	total pressure difference in the chimney [Pa]
Δp_{turb}	pressure drop across the turbine [Pa]
ε	emissivity [–]
Γ	parameter [$W m^{-2} K^{-1}$]
η_t	mechanical efficiency [–]
κ	specific heat ratio [–]
ρ, ρ_0, ρ_t	air density, ambient air density, air density inside the chimney [$kg m^{-3}$]
σ	Stefan–Boltzmann constant, 5.67×10^{-8} [$W m^{-2} K^{-4}$]
τ	shear stress [Pa]
τ_1, τ_2, τ_3	first, second cover and transparent plastic film transmissivity [–]
τ_a	transmittance considering only absorption losses [–]
τ_r	transmittance of initially unpolarized radiation [–]

Manzanares to large power plants (5, 30 and 100 MW) Yan et al. (1991) reported on a more comprehensive analytical model in which practical correlations were used to derive equations for the airflow rate, air velocity, power output and the thermo-fluid efficiency. The presented model considers the turbine of a solar chimney as a free wind turbine that, in reality, will deflect the wind, even before the wind reaches the rotor plane. The presented maximum theoretical efficiency of 16/27 (or 59%, Betz' law) does not apply for the turbines of solar chimneys. Padki and Sherif (1992) discussed in brief the effects of the geometrical and operating parameters on the chimney performance. Sampayo (1986) suggested the use of a multi-cone diffuser on the top of the chimney to allow the operation as a high-speed chimney and of acting as a draft tube for any natural wind blowing. Pasumarthi and Sherif (1997) conducted a study to demonstrate that solar chimney technology is a viable alternative energy technology suitable and adaptable to hot climate areas such as those of Florida. A mathematical model was developed to estimate the temperature and power output of solar chimneys as well as to examine the effect of various ambient conditions and structural dimensions on the power output. Tests were conducted on a demonstration model, which was design for that purpose. Two types of collectors were tested: (1) extending the collector base and (2) introducing an intermediate absorber. The experimental temperatures reported are higher than the theoretically predicted temperatures. The authors explain that one of the reasons for this behavior is the fact that the experimental temperatures reported are the maximum temperatures

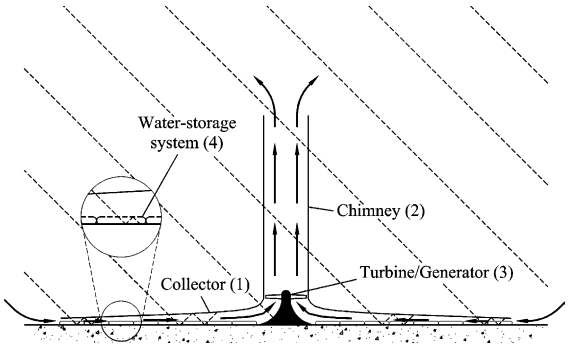

Fig. 1. Schematic drawing of a solar chimney.

attained inside the chimney, whereas the theoretical model predicts the bulk air temperature. Kreetz (1997) presented a numerical model for the use of water storage in the collector. His calculations showed the possibility of a continuous day and night operation of the solar chimney. Bernardes et al. (1999) presented a theoretical analysis of a solar chimney, operating on natural laminar convection in steady state. In order to predict thermo-hydrodynamic behaviour of air, temperature conditions were imposed on entrance, so as to guarantee steady laminar flow along the device. The mathematical model was analyzed by the method of Finite Volumes in Generalized Coordinates. Backström and Gannon (2000) presented a one-dimensional compressible flow approach for the calculation of all the thermo-dynamic variables as dependence on chimney height, wall friction, additional losses, internal drag and area exchange. Gannon and Backström (2000) developed an analysis of the solar chimney including chimney friction, system turbine, exit kinetic losses and a simple model of the solar collector. The use of solar chimneys in areas as crop drying and ventilation is considered beyond the scope of the present work.

2. Analysis

The power output of a solar chimney depends on parameters such as the ambient conditions (insolation, ambient temperature, and wind velocity) and dimensions of the chimney and collector. The analysis described in this paper is based on the following simplifying assumptions:

- axisymmetric flow of the air in the collector, i.e., nonuniform heating of the collector surface in terms of the sun's altitude angle is neglected;
- the collector is placed over a plain surface;
- the flow in the collector is considered as a flow between two parallel plates;
- the heat losses through the wall of the chimney are neglected;
- the flowing humid air is considered as a mixture of two ideal gases.

2.1. Collector

In this part of the analysis the temperature rise in the collector section is determined. This is accomplished by assuming an initial mass flow rate, while computing the final value by employing iterative techniques. The collector is considered as a cavity between two parallel plates.

2.2. Thermal network

The collector of a solar chimney is a solar air heater, which consists of an array of interconnected short solar heat collectors. Applying the momentum equation across a differential section of the collector yields

$$\frac{\partial(mu)}{\partial t} = -\dot{m}u_2 + \dot{m}u_1 + p_1A_1 - p_2A_2 - 2\pi r r_c \tau \tag{1}$$

where τ is the shear stress acting on the air in contact with the collector surface (Fig. 2).

Two types of solar collectors can be used in a solar chimney:

(I) Single channel with air flow between top glass and bottom absorber.
(II) Double channel design with single air flow between absorber and bottom covers.

Both types can be provided with the water storage system in channel where the air flows on the ground (Fig. 3). For type (II), the following heat balance equations are obtained from the thermal network at the points considering the thermal contact resistance

$$T_{f1}: S_1 + h_{r21}(T_2 - T_1) + h_1(T_{f1} - T_1) = h_w(T_1 - T_\infty) + h_{rs}(T_1 - T_s) \tag{2}$$

$$T_{f1}: h_1(T_1 - T_{f1}) = h_2(T_{f1} - T_2) \tag{3}$$

$$T_2: S_2 + h_2(T_{f1} - T_2) = h_3(T_2 - T_{f2}) + h_{r32}(T_2 - T_3) + h_{r21}(T_2 - T_1) \tag{4}$$

$$T_{f2}: h_3(T_2 - T_{f2}) = h_4(T_{f2} - T_3) + q \tag{5}$$

$$T_3: S_3 = h_4(T_3 - T_{f2}) + h_{r32}(T_3 - T_2) + h_5(T_3 - T_{f3}) + h_{r43}(T_4 - T_3) \tag{6}$$

$$T_{f3}: h_5(T_3 - T_{f3}) = h_6(T_{f3} - T_4) \tag{7}$$

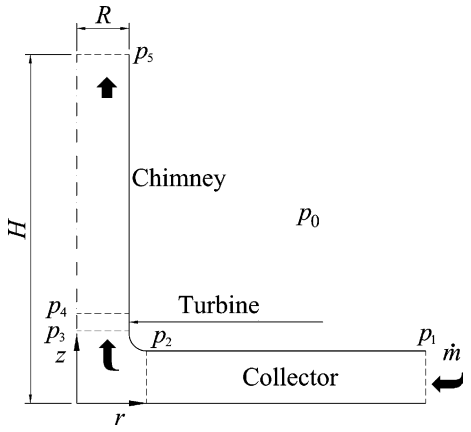

Fig. 2. Sketch of the flow in a solar chimney.

$$T_4 : S_4 = h_6(T_4 - T_{f3}) + h_{r43}(T_4 - T_3) + h_7(T_4 - T_{f4}) + U_w(T_4 - T_{4,0}) \quad (8)$$

$$T_{f4} : h_7(T_7 - T_{f4}) = h_8(T_{f4} - T_5) \quad (9)$$

$$T_5 : h_8(T_{f4} - T_5) = U_b(T_5 - T_{5,0}) \quad (10)$$

where h_1, h_2, h_3, h_4, h_5, h_6, h_7 and h_8 are the heat transfer convection coefficients of the second cover, first cover, first cover to air stream, transparent plastic film to air stream, transparent plastic film to water, absorber to water, absorber to air, ground surface to air respectively. h_{r21}, h_{r32} and h_{r43} are the radiation heat transfer coefficients between the 2nd and the 1st covers, between the first cover and the transparent plastic film and between the transparent plastic film and absorber respectively. T_1, T_2, T_3, T_4, T_5, T_b represent the temperatures at the second cover, first cover, transparent plastic film, absorber, ground surface and ground temperatures, respectively. T_{f1}, T_{f2}, T_{f3}, T_{f4} represent the air temperature between second and first cover, mean air temperature, water temperature and the air temperature between absorber and ground surface respectively. U_b, U_t, and U_w represent the heat transfer coefficient at the ground, the top loss heat coefficient and the heat transfer coefficient in the water storage system respectively.

By assuming that the air temperature varies linearly along each collector section, the mean temperature is then equal to the arithmetic mean

$$T_f = \frac{(T_{f,i} - T_{f,o})}{2} \quad (11)$$

The useful heat transferred to the moving air stream can be written in terms of the mean fluid and inlet temperature as

$$q = \Gamma(T_f - T_{f,i}) \quad (12)$$

where

$$\Gamma = \dot{m}c_p/\pi rL \quad (13)$$

By substituting Eq. (12) into Eq. (4) and rearranging we obtain:

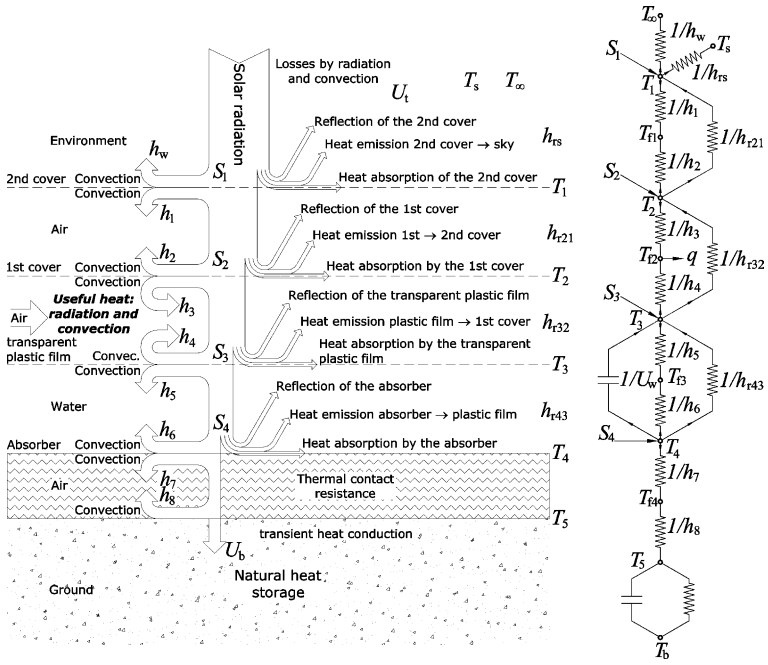

Fig. 3. Thermal network for the collector of solar chimneys.

- a 9×9 matrix (Eq. (14)) for the type (II) collector with water storage,
- a 7×7 matrix (Eq. (15)) for the type (I) with water storage,
- a 7×7 matrix (Eq. (16)) for the type (II) without water storage and
- a 5×5 matrix (Eq. (17)) for the type (I) without water storage.

$$\begin{bmatrix}
\begin{pmatrix} h_1 \\ +h_{r21} \\ +U_t \end{pmatrix} & -h_1 & -h_{r21} & 0 & 0 & 0 & 0 & 0 & 0 \\
h_1 & -\begin{pmatrix} h_1 \\ +h_2 \end{pmatrix} & h_2 & 0 & 0 & 0 & 0 & 0 & 0 \\
-h_{r21} & -h_2 & \begin{pmatrix} h_2 \\ +h_3 \\ +h_{r21} \\ +h_{r32} \end{pmatrix} & -h_3 & -h_{r32} & 0 & 0 & 0 & 0 \\
0 & 0 & h_3 & -\begin{pmatrix} h_3 \\ +h_4 \\ +\Gamma \end{pmatrix} & h_4 & 0 & 0 & 0 & 0 \\
0 & 0 & -h_{r32} & -h_4 & \begin{pmatrix} h_4 \\ +h_{r32} \\ +h_{r43} \\ +h_5 \end{pmatrix} & -h_5 & -h_{r43} & 0 & 0 \\
0 & 0 & 0 & 0 & h_5 & -\begin{pmatrix} h_5 \\ +h_6 \end{pmatrix} & h_6 & 0 & 0 \\
0 & 0 & 0 & 0 & -h_{r43} & -h_6 & \begin{pmatrix} h_6 \\ +h_{r43} \\ +h_7 \\ +U_w \end{pmatrix} & -h_7 & 0 \\
0 & 0 & 0 & 0 & 0 & 0 & h_7 & -\begin{pmatrix} h_7 \\ +h_8 \end{pmatrix} & h_8 \\
0 & 0 & 0 & 0 & 0 & 0 & 0 & -h_8 & \begin{pmatrix} h_8 \\ +U_b \end{pmatrix}
\end{bmatrix}
\begin{bmatrix} T_1 \\ T_{f1} \\ T_2 \\ T_{f2} \\ T_3 \\ T_{f3} \\ T_4 \\ T_{f4} \\ T_5 \end{bmatrix}
=
\begin{bmatrix} S_1 + h_w T_\infty + h_{rs} T_s \\ 0 \\ S_2 \\ -\Gamma T_{f2,i} \\ S_3 \\ 0 \\ S_4 + U_w T_{4,0} \\ 0 \\ U_b T_{5,0} \end{bmatrix} \tag{14}$$

$$\begin{bmatrix}
\begin{pmatrix} h_3 \\ +h_{r21} \\ +U_t \end{pmatrix} & -h_3 & -h_{r32} & 0 & 0 & 0 & 0 \\
h_3 & -\begin{pmatrix} h_3 \\ +h_4 \\ +\Gamma \end{pmatrix} & h_4 & 0 & 0 & 0 & 0 \\
-h_{r32} & -h_4 & \begin{pmatrix} h_4 \\ +h_{r32} \\ +h_{r43} \\ +h_5 \end{pmatrix} & -h_5 & -h_{r43} & 0 & 0 \\
0 & 0 & h_5 & -\begin{pmatrix} h_5 \\ +h_6 \end{pmatrix} & h_6 & 0 & 0 \\
0 & 0 & -h_{r43} & -h_6 & \begin{pmatrix} h_6 \\ +h_{r43} \\ +h_7 \\ +U_w \end{pmatrix} & -h_7 & 0 \\
0 & 0 & 0 & 0 & h_7 & -\begin{pmatrix} h_7 \\ +h_8 \end{pmatrix} & h_8 \\
0 & 0 & 0 & 0 & & -h_8 & \begin{pmatrix} h_8 \\ +U_b \end{pmatrix}
\end{bmatrix}
\begin{bmatrix} T_2 \\ T_{f2} \\ T_3 \\ T_{f3} \\ T_4 \\ T_{f4} \\ T_5 \end{bmatrix}
=
\begin{bmatrix} S_2 + h_w T_\infty + h_{rs} T_s \\ -\Gamma T_{f2,i} \\ S_3 \\ 0 \\ S_4 + U_w T_{4,0} \\ 0 \\ U_b T_5, 0 \end{bmatrix} \tag{15}$$

$$\begin{bmatrix} \begin{pmatrix} h_1 \\ +h_{r21} \\ +U_t \end{pmatrix} & -h_1 & -h_{r21} & 0 & 0 & 0 & 0 \\ h_1 & -\begin{pmatrix} h_1 \\ +h_2 \end{pmatrix} & h_2 & 0 & 0 & 0 & 0 \\ -h_{r21} & -h_2 & \begin{pmatrix} h_2 \\ +h_3 \\ +h_{r21} \\ +h_{r23} \end{pmatrix} & -h_3 & -h_{r32} & 0 & 0 \\ 0 & 0 & h_3 & -\begin{pmatrix} h_3 \\ +h_4 \\ +\Gamma \end{pmatrix} & h_4 & 0 & 0 \\ 0 & 0 & -h_{r32} & -h_4 & \begin{pmatrix} h_4 \\ +h_{r32} \\ +h_7 \end{pmatrix} & -h_7 & 0 \\ 0 & 0 & 0 & 0 & h_7 & -\begin{pmatrix} h_7 \\ +h_8 \end{pmatrix} & h_8 \\ 0 & 0 & 0 & 0 & 0 & -h_8 & \begin{pmatrix} h_8 \\ +U_b \end{pmatrix} \end{bmatrix} \begin{bmatrix} T_1 \\ T_{f1} \\ T_2 \\ T_{f2} \\ T_4 \\ T_{f4} \\ T_5 \end{bmatrix} = \begin{bmatrix} S_1 + h_w T_\infty + h_{rs} T_s \\ 0 \\ S_2 \\ -\Gamma T_{f2,1} \\ S_3 \\ 0 U_b T_{5,0} \end{bmatrix} \tag{16}$$

$$\begin{bmatrix} (h_3 + h_{r32} + U_t) & -h_3 & -h_{r32} & 0 & 0 \\ h_3 & -(h_3 + h_4 + \Gamma) & h_4 & 0 & 0 \\ -h_{r32} & -h_4 & (h_4 + h_{r32} + h_7) & -h_7 & 0 \\ 0 & 0 & h_7 & -(h_7 + h_8) & h_8 \\ 0 & 0 & 0 & -h_8 & (h_8 + U_b) \end{bmatrix} \begin{bmatrix} T_2 \\ T_{f2} \\ T_4 \\ T_{f4} \\ T_5 \end{bmatrix} = \begin{bmatrix} S_2 + h_w T_\infty + h_{rs} T_s \\ -\Gamma T_{f2,i} \\ S_3 \\ 0 \\ U_b T_{5,0} \end{bmatrix} \tag{17}$$

In general, the above matrices may be written as

$$[A][T] = [B] \tag{18}$$

The mean temperature vector may be determined by matrix inversion

$$[T] = [A]^{-1}[B] \tag{19}$$

2.3. Heat transfer coefficients

The overall top heat loss coefficient may be obtained from

$$U_t = (h_w + h_{rs}) \tag{20}$$

with

$$h_w = \frac{k}{L} Nu \tag{21}$$

and

$$h_{rs} = \frac{\sigma \varepsilon (T_1 + T_s)(T_1^2 + T_s^2)(T_1 - T_s)}{(T_1 - T_\infty)} \tag{22}$$

The clean sky temperature T_s obtained by Berdahl and Martin (1984) is given by

$$T_s = T_\infty [0.711 + 0.0056(T_{dp} - 273.15) + 0.000073(T_{dp} - 273.15)^2 + 0.013\cos(15t)]^{1/4} \tag{23}$$

where t is the hour from midnight.

The ground heat transfer coefficient is given by

$$U_b = \frac{2b}{\sqrt{\pi t}} \tag{24}$$

with

$$b = \sqrt{k \rho c_p} \tag{25}$$

The radiation heat transfer coefficients between two parallel plate sets 1–2, 2–3 and 3–4 are given as

$$h_{r21} = \frac{\sigma (T_1^2 + T_2^2)(T_1 + T_2)}{\left(\frac{1}{\varepsilon_1} + \frac{1}{\varepsilon_2} - 1\right)} \tag{26}$$

$$h_{r32} = \frac{\sigma(T_2^2 + T_3^2)(T_2 + T_3)}{\left(\frac{1}{\varepsilon_2} + \frac{1}{\varepsilon_3} - 1\right)} \quad (27)$$

$$h_{r43} = \frac{\sigma(T_3^2 + T_4^2)(T_3 + T_4)}{\left(\frac{1}{\varepsilon_3} + \frac{1}{\varepsilon_4} - 1\right)} \quad (28)$$

The solar radiation heat fluxes absorbed by the surfaces are

$$S_1 = \alpha_1 H \quad (29)$$

$$S_2 = \tau_1 \alpha_2 H \quad (30)$$

$$S_3 = \tau_2 \alpha_3 H \quad (31)$$

$$S_4 = \tau_3 \alpha_4 H \quad (32)$$

where S_1, S_2, S_3 represents the solar radiation absorbed by the second cover, by the first cover, by the transparent plastic film, by absorber, respectively.

The transmittance and the absorptivity of a single cover is

$$\tau \cong \tau_a \tau_r \quad (33)$$

$$\alpha \cong 1 - \tau_a \quad (34)$$

Eqs. (33) and (34) can be used for a two-cover system if the covers are identical (Duffie and Beckman, 1991).

To solve the problem of non-stationary heat condition in the water-storage system we consider a homogeneous boundary-value problem for an infinitely wide plane slab with a prescribed boundary temperature. The temperature and the heat flux density distributions are determined analytically. The heat transfer coefficient of the water-storage system can be calculated by

$$U_w = \frac{q_{01}}{\Delta\vartheta} = \frac{1}{t}\sum_{k=0}^{\infty}\left[\frac{2L_w \sin(\delta_k)^2}{\alpha\delta_k[\delta_k + \sin(\delta_k)\cos(\delta_k)]} e^{\left(-\delta_k^2 \alpha \frac{t_1}{L_w^2}\right)}\right] \quad (35)$$

with $\delta_1 = \pi/2$, $\delta_2 = 3\pi/2$, $\delta_3 = 5\pi/2, \ldots$, $\delta_k = (k - 1/2)\pi$.

Table 1 shows a list of correlations employed for forced (h_1–h_8) and natural convection coefficients (h_w). The subscriptions m,lam, m,turb and x represents the mean laminar, mean turbulent and local Nusselt number.

2.4. Friction loss in the collector

Table 2 shows the employed friction factors to calculate the shear stress in the collector.

2.5. Chimney

The chimney converts the thermal energy produced by the solar collector into kinetic energy. The density difference created by the rise in temperature in the collector works as the driving force. The heat transfer taking place across the chimney section surface is negligible. Applying the momentum equation across a differential section of the chimney yields

Table 1
Correlations employed for forced and natural convection (flat plate, constant temperature)

Equations		Flow regime/source
Forced convection		
$Nu_m = \frac{1}{\sqrt{\pi}}\sqrt{Re_x}\frac{\Pr}{(1 + 1.7\Pr^{1/4} + 21.36\Pr)^{1/6}}$	(36)	Laminar, $Re < 5 \times 10^5$, Baehr and Stephan (1996)
$Nu_{m,lam} = 2Nu_x$		
$Nu_m = \frac{0.037 Re^{0.8}\Pr}{1 + 2.443 Re^{-0.1}(\Pr^{2/3} - 1)}$	(37)	$5 \times 10^5 < Re < 10^7$ $0.6 < Pr < 2000$ Petukhov and Popov (1963)
$Nu_m = \sqrt{Nu_{m,lam}^2 + Nu_{m,tur}^2}$	(38)	Schlichting et al. (1999)
Free convection		
$Nu_m = 0.54 Ra^{1/4}$	(39)	$10^4 \leqslant Ra < 10^7$, upper or lower heated horizontal surface, Churchill and Chu (1975)
$Nu_m = 0.14 Ra^{1/3}$	(40)	$10^7 \leqslant Ra \leqslant 10^{11}$, upper or lower heated horizontal surface, Churchill and Chu (1975)

Table 2
Correlations employed for the shear stress in the collector (flat plate)

Equations		Flow regime/Source
$\frac{c_w}{2} = \frac{0.664}{\sqrt{Re_L}}$	(41)	Laminar, smooth Baehr and Stephan (1996)
$\frac{c_w}{2} = \frac{0.0592}{Re_L^{1/5}}$	(42)	Turbulent, smooth, $10^5 \leqslant Re_L \leqslant 10^7$, Baehr and Stephan (1996)
$c_w = \frac{0.072}{Re_L^{1/5}} - \frac{1700}{Re_L}$	(43)	Transition, smooth, Schlichting et al. (1999)
$c_w = \left[1.89 - 1.62\log\left(\frac{k_r}{L}\right)\right]^{-2.5}$	(44)	Turbulent, rough, $10^{-6} < k_r/L < 10^{-2}$, Schlichting et al. (1999)

Table 3
Correlations employed for the shear stress in the chimney (tube, smooth)

Equations		Flow regime/source
$f = \frac{16}{Re}$	(45)	Laminar, fully developed $Re \leqslant 2100$ Baehr and Stephan (1996)
$\frac{1}{\sqrt{f}} = 1.5635\ln\left(\frac{Re}{7}\right)$	(46)	Turbulent, fully developed $4000 < Re < 10^7$ Colebrook (1939)
$\frac{2}{f} = \left\{\frac{1}{[(8/Re)^{10} + (Re/36500)^{20}]^{1/2}} + \left[2.21\ln\left(\frac{Re}{7}\right)\right]^{10}\right\}^{1/5}$	(47)	Turbulent, rough $10^{-6} < k_r/L < 10^{-2}$ Schlichting et al. (1999)

$$\frac{d\rho w^2}{dz} = \frac{dp}{dz} - (\rho - \rho_0)g \tag{48}$$

Thus, the velocity can be expressed as

$$w = \sqrt{\frac{2}{\rho}\left[\int_0^{H_k}(\rho_0 - \rho)g\,dz - \Delta p_{friction}\right]} \tag{49}$$

Outside of the chimney, pressure, temperature and density variation of air is calculated considering the standard atmosphere

$$T_\infty(z) = T_\infty(0)\left(1 - \frac{\kappa - 1}{\kappa}\frac{z}{H_0}\right) \tag{50}$$

$$p_\infty(z) = p_\infty(0)\left(1 + \frac{\kappa - 1}{\kappa}\frac{z}{H_0}\right)^{\kappa/(\kappa-1)} \tag{51}$$

$$\rho_\infty(z) = \rho_\infty(0)\left(1 + \frac{\kappa - 1}{\kappa}\frac{z}{H_0}\right)^{1/(\kappa-1)} \tag{52}$$

with

$$H_0 = \frac{R_l T_\infty(0)}{g} \tag{53}$$

and $\kappa = 1.235$ (standard atmosphere).

Pressure, temperature and density variation of air inside the chimney is calculated considering an adiabatic expansion process. Thus

$$T_t(z) = T_{t,in}(0)\left(1 - \frac{\kappa - 1}{\kappa}\frac{z}{H_0}\right) \tag{54}$$

$$p_t(z) = p_t(0)\left(1 + \frac{\kappa - 1}{\kappa}\frac{z}{H_0}\right)^{\kappa/(\kappa-1)} \tag{55}$$

$$\rho_t(z) = \rho_t(0)\left(1 + \frac{\kappa - 1}{\kappa}\frac{z}{H_0}\right)^{1/(\kappa-1)} \tag{56}$$

with

$$H_0 = \frac{R_l T_{t,in}}{g} \tag{57}$$

and $\kappa = 1.4005$.

2.6. Friction loss in the chimney

Table 3 shows the employed friction factors to calculate the shear stress in the chimney.

2.7. Turbine and generator

The heat flow produced by the collector is converted into kinetic energy (convection current) and potential energy (pressure drop at the turbine) through the chimney. Thus, the density difference of the air caused by the temperature rise in the collector work as a driving force. The lighter column of air in the chimney is connected with the surrounding atmosphere at the base (inside the collector) and at the top of the chimney, and thus acquires lift. Between chimney base (collector outflow) and the surroundings a pressure difference Δp_{tot} is produced. The pressure drop across the turbine can be expressed as a function of the total pressure difference

$$\Delta p_{\text{turb}} = \Delta p_{\text{tot}} - \frac{1}{2}\rho w^2 \tag{58}$$

with

$$\Delta p_{\text{tot}} = \int_0^{H_k} (\rho_0 - \rho) g \, \mathrm{d}z \tag{59}$$

The velocity at the exit of the chimney can be found using

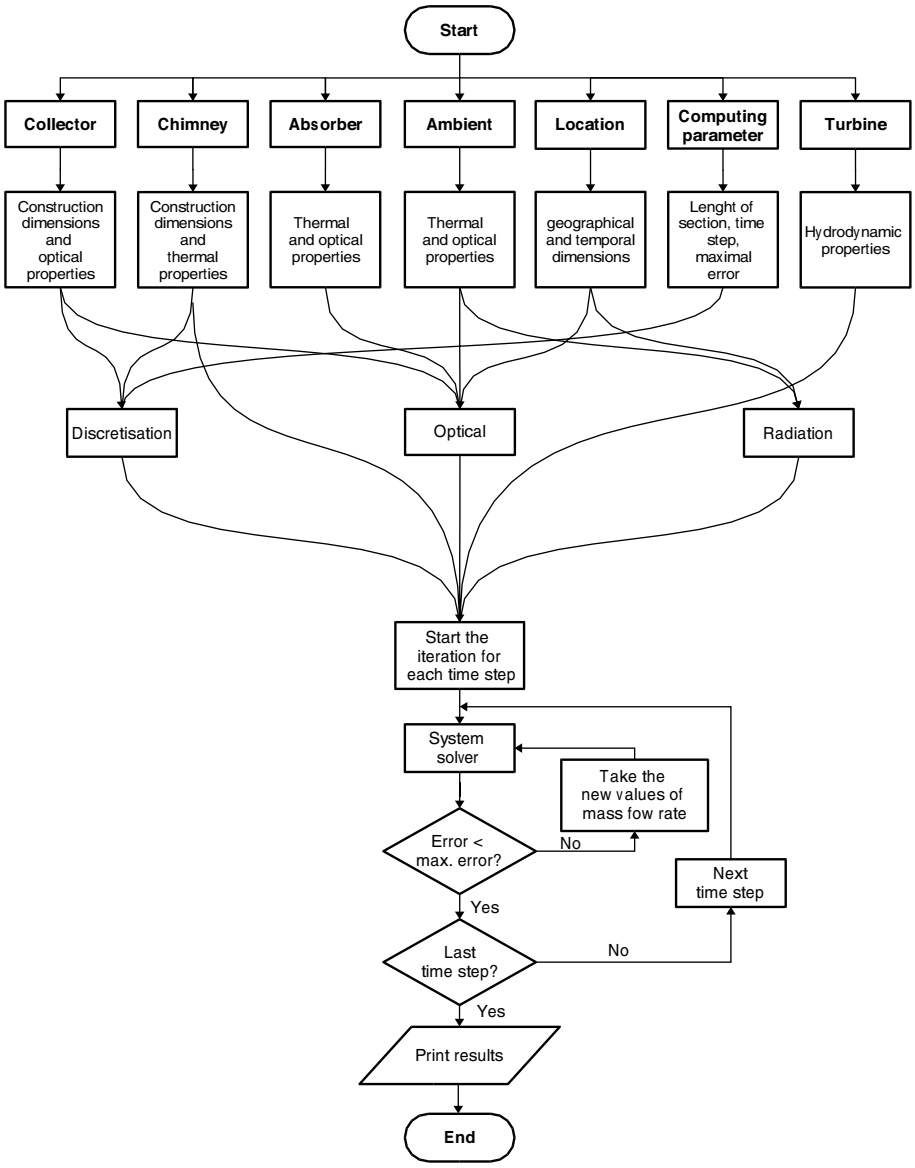

Fig. 4. Flowchart for computer programm.

$$w = w_{tot}\sqrt{1-x} \tag{60}$$

where x is the factor of pressure drop at the turbine and w_{tot} is the velocity obtained neglecting friction losses.

The theoretical utilisable power taken up by the turbine is

$$P = \Delta p_{tot} A w_{tot} \eta_t x \sqrt{1-x} \tag{61}$$

2.8. Solar radiation

The incident solar energy has three different spatial distributions: beam radiation, diffuse sky radiation, and ground-reflected radiation. In the presented model, the incident radiation can be calculated by available procedures (for example: Duffie and Beckman, 1991) or read from a file. Both procedures are not described in this paper.

2.9. Physical properties

The physical properties of air and water used in this work are calculated by interpolation of data from standard tables (for example: VDI-Wärmeatlas, 1997).

3. Theoretical solution procedure

The computer program is outlined in the flowchart shown in Fig. 4. The theoretical model assumes that for a short collector, the temperatures of the "boundaries" surrounding the air streams are uniform and the temperatures of the air streams vary linearly along the collector. A long collector can be assumed to be divided equally into a finite number of short collectors, or sections. The wall and mean air temperatures of the first section are equal to the ambient temperature. Heat transfer coefficients are evaluated according to the initially guessed values. An iterative process is then created and the mean temperatures for the section calculated using the equations derived by employing a standard package matrix-inversion. The iterative process is repeated until all consecutive mean temperatures differ by less then a desired value.

Another section of collector, with length equal to the previous section, is then added to the end of the first section. The mean wall and air temperatures of the second section of collector are then set equal to the mean wall temperature and air temperature of the section before it. The inlet air temperature of the second section is set equal to the outlet temperature of the first section. The iterative procedure is repeated until all the sections of the given collector are considered. By this procedure, wall and mean air temperature can be predicted for the complete length of collector.

The start of the program considers the first section of the collector. An initial guess of the mass flow rate is made. An iterative process is then initiated. The programme calculates all the required heat transfer and friction loss coefficients based on the initially guessed temperatures and mass flow rate. Each new mass flow rate value calculated in the chimney is then compared with the old corresponding value. If the difference between any corresponding new and old values is less then the maximal acceptable difference, the iteration is stopped. The programme then proceeds to look at the next time step. At the end of the iteration, the programme calculates the outlet temperatures of the air streams at the end of the current section of the collector and chimney. By this repetitive and iterative process, the required temperatures along the entire length of the collector and height of the chimney, and also the mass flow rate, generated power in the turbine, etc. can be obtained.

4. Validation of the mathematical model

To validate the mathematical model, the theoretical performance data obtained by the program were compared with the experimental data of the prototype from Manzanares, Spain (06/07/1987 and 06/08/1987). The plant was equipped with extensive measurement data acquisition facilities. The performance of the plant was registered considering a time step of one second and using 180 sensors (Schiel, 2002). In addition to the

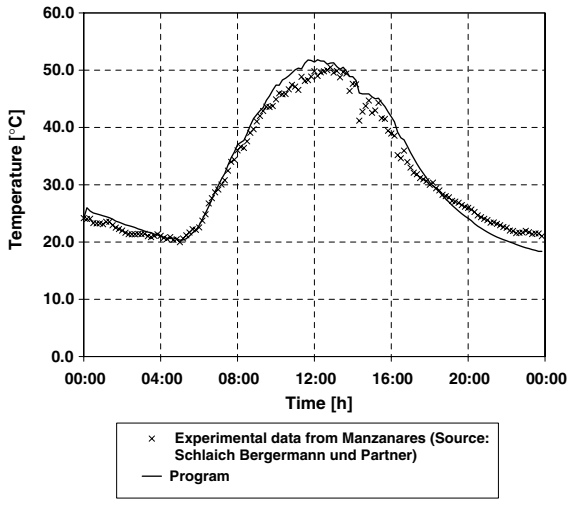

Fig. 5. Air temperature in collector during the day ($R_c = 48$ m—06/07/1987).

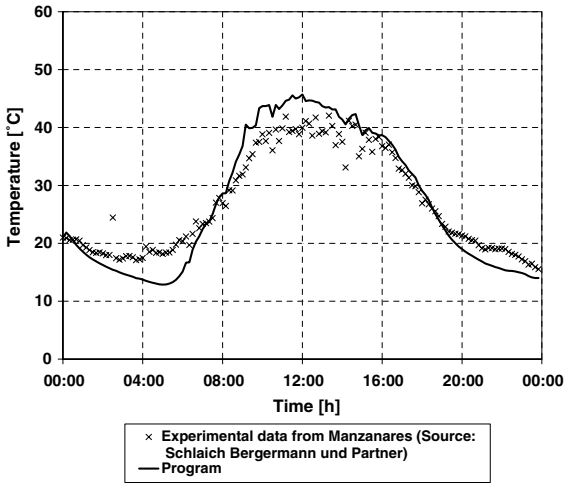

Fig. 6. Air temperature in collector during the day ($R_c = 48$ m—06/08/1987).

Table 4
Comparison between theoretical and the experimental data of production of energy [kW h]

	06/07/1987	06/08/1987
Experimental data from Manzanares (Schiel, 2002)	268.0	366.8
Program	273.1	360.7
Divergence [%]	1.9	−1.6

dimensions, the following meteorological data were used to simulate the prototype:

- solar radiation;
- air temperature in dependency on the height;
- relative air humidity;
- wind velocity;
- factor of pressure drop at the turbine.

Figs. 5 and 6 show a comparison among theoretical and experimental air temperature inside the collector during the day. An agreement within 2% of the electric power output was obtained with the present theoretical model (Table 4).

5. Sensitivity analysis

The mathematical model was developed to estimate the temperature and power output of solar chimneys as well as to examine the effect of various ambient conditions and structural dimensions on the power output. It is recognized that the power generation of the solar chimney is proportional to the volume included within the chimney height and the collector area. Thus, the same output can be achieved with different combinations of geometries. There is no physical optimum. Optimal dimensions can determined by including the cost of the system at a particular site. The influence of the following parameters was analysed

- *Chimney height* (500–1250 m). Schlaich (1995) mentioned that chimneys 1000 m high can be built without difficult and that serious plans are being made for 2000 m skyscrapers in earthquake-ridden in Japan.
- *Collector area* (9.6–19.6 km^2). A flat collector can convert up to 70% of irradiated solar energy into heat.
- *Double cover area* (0–100% of collector area). Theoretically, it is advantageous to increase the ability of the collector roof to retain heat as the temperature increases from the perimeter towards the tower. This can be done by providing double glazing near the tower.
- *Water-storage system area* (0–100% of collector area) *and thickness* (0–0.150 m). This parameter examines the feasibility of a water storage system for the solar chimney.
- *Cover optical properties* (transmittance: 0.50–0.95). In arid zones dust and sand inevitably collect on the collector roof and of course reduce its efficiency.
- *Ground heat penetration coefficient* (1000–2000 W s$^{1/2}$/K m^2). The ground under the roof provides natural thermal storage.
- *Distance between absorber and ground* (0–0.10 m). In order to adequately model and design the collector, a knowledge of the thermal contact resistance between the absorber and the ground is crucial.
- *Factor of pressure drop at the turbine* (0.5–0.99). This factor represents the fraction of the total difference of pressure in the system, which drops at the turbine. The turbine is generally designed so that they yield maximum output at variable air speeds and is therefore designed with some sort of power control. There are many different ways of doing this safely on modern wind turbines: pitch, stall, active stall control and ailerons (older turbines).

Table 5 presents the used initial parameters.

Figs. 7 and 8 presents the variation of the power output as a function of different parameters. The influence of the chimney height, collector area, cover optical properties and factor of pressure drop at the turbine are substantial. With an increase in chimney height, the pressure drop across the chimney increases. This results in an increase in velocity and an associated increase in the mass flow rate and the power output. The increase in the collector area and transmittance causes an increase

Table 5
Data to the sensitivity analysis

Parameter	Value	Unit
Collector height at entrance	3.5	m
Collector height at exit	35	m
Collector diameter	4100	m
Cover material	Glass	–
Cover refractive index	1.526	–
Cover emissivity	0.90	–
Cover extinction coefficient	23.6	m^{-1}
Cover thickness	0.004	m
Chimney diameter at entrance	120	m
Chimney diameter at exit	120	m
Chimney height	1000	m
Absorber absorptivity	0.93	–
Absorber emittance	0.90	–
Water-storage system thickness	0.10	m
Water-storage system absorptivity	0.90	[–]
Water-storage system emittance	0.90	[–]
Water-storage system transmittance	0.10	[–]
Distance absorber/ground	1.0×10^{-6}	m
Ground roughness	0.05	m
Ground thermal conductivity	0.6	$W/m^{-1}\,K^{-1}$
Ground thermal diffusivity	2.91×10^{-7}	$m^2\,s^{-1}$
Latitude	0	deg
Longitude	−20 (East)	deg
Date	01.06.2001	–
Maximum error for solver	0.1	%
Number of radial collector sections	300	–
Time step	1800	s
Factor of pressure drop	0.90	–
Efficiency of turbine/generator	0.75	–

in the collector exit temperatures, thus resulting in an increase mass flow rate, and hence an increase power output. The maximum power is drawn when the factor of pressure drop at the turbine is equal to approximately 0.97. The throttling ($x \to 1$) reduces the air flow in the system and, consequently, the air temperature rises in the collector, increasing the total pressure difference Δp_{tot} in Eq. (59) (Fig. 9). In reality, a factor of pressure drop at the turbine equal to 0.97 is hard to be achieved.

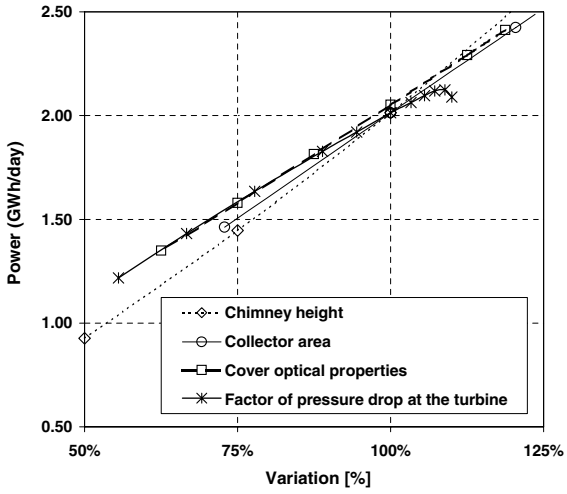

Fig. 7. Power output by variation of different parameters.

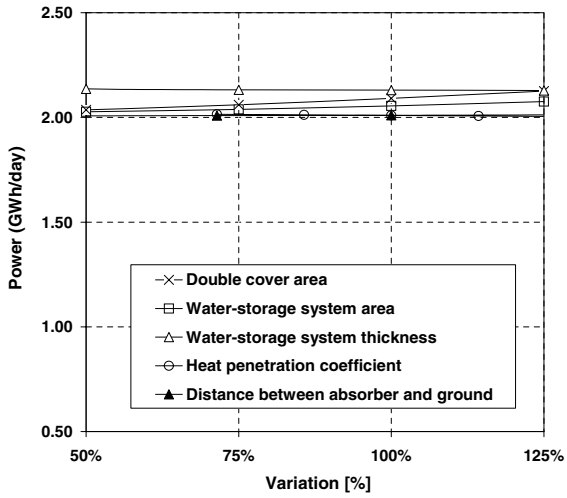

Fig. 8. Power output by variation of different parameters.

Thus, the use of a value between 0.80 and 0.90 is recommended.

The effect of the thickness and area of water-storage system on the power production are show in Figs. 10 and 11. As can be seen, the use of this system increases the power production at night. The variation of the ground property heat penetration coefficient, double cover area and distance between absorber and ground presented no significant variations.

6. Conclusions

The objective of this study was to evaluate the solar chimney performance theoretically. A mathematical

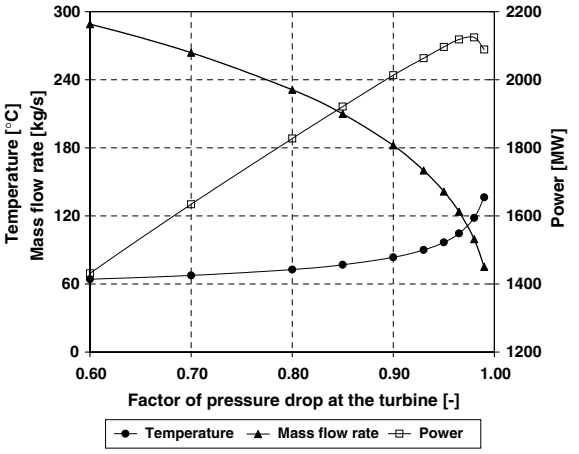

Fig. 9. Temperature and power output as function of the factor of pressure drop at the turbine.

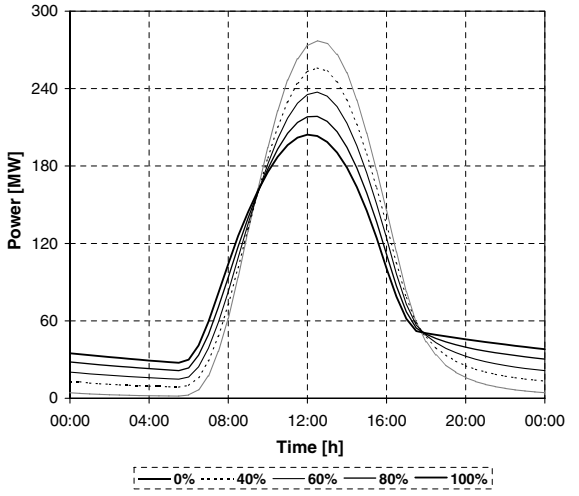

Fig. 10. Effect of the use of water-storage system as a function of covered collector area on the power production.

model was developed to estimate the temperature and power output of solar chimneys as well as to examine the effect of various construction conditions on the power output. The mathematical model was validated with the experimental data from the prototype in Manzanares. The power output can be increased by increasing the chimney height, the collector area and the transmittance of the collector. The maximum power can be reached when the factor of pressure drop at the turbine is equal to approximately 0.97. Other parameters such as ground heat penetration coefficient, distance between absorber and ground, double cover area, water-storage system area and thickness presented no significant variations on the energy output, but on power output vs. time.

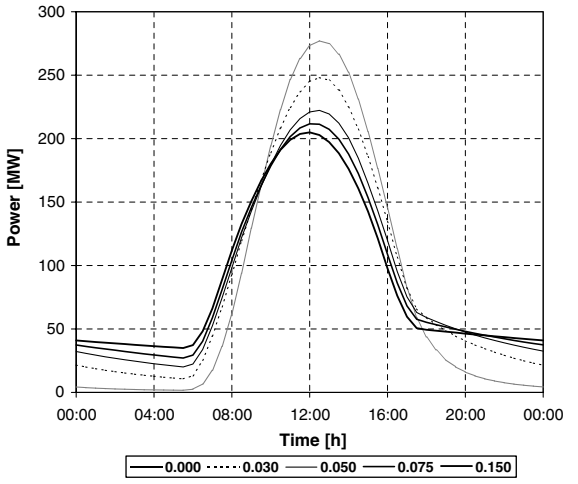

Fig. 11. Effect of the water layer thickness on power production.

References

Backström, T.W.V., Gannon, A.J., 2000. Compressible flow through tall chimneys. In: Proceedings of Solar 2000: Solar Powers Life, Share the Energy.

Baehr, H.D., Stephan, K., 1996. Wärme- und Stoffübertragung. Springer-Verlag, Berlin.

Berdahl, P., Martin, M., 1984. Emissivity of clear skies. Solar Energy 32 (5), 663–664.

Bernardes, M.A.D.S., Valle, R.M., Cortez, M.F.-B., 1999. Numerical analysis of natural laminar convection in a radial solar heater. Int. J. Therm. Sci. 38, 42–50.

Castillo, M.A., 1984. A new solar chimney design to harness energy from the atmosphere. Spirit of Enterprise: The 1984 Rolex Awards, pp. 58–59.

Churchill, S.W., Chu, H.H.S., 1975. Correlating equations for laminar and turbulent free convection from a vertical plate. Int. J. Heat Mass Transfer 18, 1323–1329.

Colebrook, C.F., 1939. Turbulent flow in pipes with particular reference to the transition region between the smooth and rough pipes law. J. Instit. Civil Eng. 11, 133–156.

Duffie, J.A., Beckman, W.A., 1991. Solar Engineering of Thermal Processes, second ed. Wiley Interscience, New York.

Gannon, A.J., Backström, T.W.V., 2000. Solar chimney cycle analysis with system loss and solar collector performance. In: Proceedings of Solar 2000: Solar Powers Life, Share the Energy.

Haaf, W., 1984. Solar chimneys, part II: preliminary test results from the Manzanares pilot plant. Int. J. Solar Energy 2, 141–161.

Haaf, W., Friedrich, K., Mayr, G., Schlaich, J., 1983. Solar chimneys, part I: principle and construction of the pilot plant in Manzanares. Int. J. Solar Energy 2, 3–20.

Kreetz, H., 1997. Theoretische Untersuchungen und Auslegung eines tempor. Diplomarbeit TU Berlin, Berlin.

Mullet, L.B., 1987. The solar chimney overall efficiency, design and performance. Int. J. Ambient Energy 8 (1), 35–40.

Padki, M.M., Sherif, S.A., 1989a. Solar chimney for medium-to-large scale power generation. In: Proceedings of the Manila International Symposium on the Development and Management of Energy Resources, Manila, Philippines, 1, pp. 432–437.

Padki, M.M., Sherif, S.A., 1989b. Solar chimney for power generation in rural areas. Seminar on Energy Conservation and Generation Through Renewable Resources, Ranchi, India, pp. 91–96.

Padki, M.M., Sherif, S.A., 1992. A mathematical model for solar chimneys. In: Proceedings of 1992 International Renewable Energy Conference, Amman, Jordan, Vol. 1, pp. 289–294.

Pasumarthi, N., Sherif, S.A., 1997. Performance of a demonstration solar chimney model for power generation. In: Proceedings of the 35th Heat Transfer and Fluid Mechanics.

Petukhov, B.S., Popov, N.V., 1963. Theoretical calculation of heat transfer and frictional resistance in turbulent flow in tubes of an incompressible fluid with variable physical properties. High Temperature 1, 69–83.

Sampayo, E.A., 1986. Solar-wind power system. Spirit of Enterprise: The 1986 Rolex Awards, pp. 3–5.

Schlaich, J., Schiel, W., Friedrich, K., Schwarz, G., Wehowsky, P., Meinecke, W., Kiera, M. 1990. Abschlußbericht Aufwindkraftwerk, Übertragbarkeit der Ergebnisse von Manzanares auf größere Anlagen, BMFT-Förderkennzeichen 0324249D, Stuttgart.

Schlaich, J., 1995. The Solar Chimney. Edition Axel Menges, Stuttgart.

Schlichting, H., Gersten, K., Krause, E., Mayes, K., Oertel, H., 1999. Boundary-Layer Theory. Springer-Verlag, Berlin.

Wärmeatlas, 1997. VDI—Wärmeatlas. Springer-Verlag, Berlin.

Schiel, W., 2002. Experimental data from the solar chimney prototype in Manzanares (Spain). Private Communications with the Büro Schlaich Bergermann und Partner.

Yan, M.-Q., Sherif, S.A., Kridli, G.T., Lee, S.S., Padki, M.M., 1991. Thermo-fluids analysis of solar chimneys. Ind. Applic. Fluid Mech. ASME FED-2, 125–130.